CHEMISTRY
A EUROPEAN JOURNAL

DOI: 10.1002/chem.200600418

Upconversion Between 4f–5d Excited States in Tm^{2+}-Doped $CsCaCl_3$, $CsCaBr_3$, and $CsCaI_3$

J. Grimm, E. Beurer, P. Gerner, and H. U. Güdel*[a]

Abstract: Near-infrared to visible upconversion luminescence in $CsCaCl_3$:Tm^{2+}, $CsCaBr_3$:Tm^{2+} and $CsCaI_3$:Tm^{2+} is presented and analysed. The upconversion process involves exclusively the 4f–5d excited states of Tm^{2+}, which is a novelty among upconversion materials. The presence of more than one long-lived 4f–5d excited state is the prerequisite for this. Multiple emissions from Tm^{2+} are observed in the title compounds. This is made possible by the favourable energy structure within the 4f–5d states and the low phonon energies of the materials. The energy positions of the relevant 4f–5d states, and thus the photophysical and light emission properties, are affected by the chemical variation along the series. The upconversion efficiency increases from chloride to iodide and the mechanism is found to be a combination of absorption and energy-transfer steps.

Keywords: laser spectroscopy · luminescence · thulium · upconversion

Introduction

Light-emitting inorganic materials that are able to emit visible (Vis) light upon excitation in the near-infrared (NIR) in a so-called upconversion (UC) process have received considerable attention in the past.[1,2] UC is a well-established and efficient nonlinear optical process. It does not require coherent pump radiation in contrast to other nonlinear optical processes like second-harmonic generation (SHG) or two-photon absorption (TPA). Since light-emitting diodes with extremely high energy efficiencies are available as pump sources in the NIR, UC processes are attractive for future technologies. As a consequence, UC materials are investigated for application as lasing media,[3] for application in displays,[4] for use in immunoassays and bio-labelling[5] as well as for improving the efficiency of solar cells.[6]

A second fundamental difference of UC with respect to SHG and TPA is that UC requires at least two metastable excited states. This basic prerequisite reduces the number of potential upconversion systems, because the majority of light-emitting materials have just one emissive state, usually the first excited state. Exceptions are most trivalent lanthanides. Thus, it is not surprising that the vast majority of UC studies involve the 4f–4f transitions of lanthanide-doped materials.[1] In addition, a few upconversion systems based on d–d transitions in transition-metal-doped materials exist.[7–9] However, UC is not restricted to transitions within the 4f states of lanthanides, the d states of transition metals or a combination of both. Any luminescent material that exhibits multiple emissions is a potential candidate for UC.

Recent investigations of the optical spectroscopic properties of Tm^{2+} revealed that this ion is capable of emitting light from more than one excited state. The number of observed Tm^{2+} transitions is highly dependent on the host lattice.[10–13] In all lattices, a sharp and long-lived 4f–4f emission is found in the NIR region. At higher energies, broad and fast decaying emission bands are observed that originate from the 4f–5d states of Tm^{2+}. UC between 4f–4f and 4f–5d states was demonstrated a few years ago in $SrCl_2$:Tm^{2+}.[12] A new type of UC process involving exclusively the 4f–5d states of Tm^{2+} was reported recently for $CsCaI_3$:Tm^{2+}.[14] In the present contribution, an extended study on the entire $CsCaX_3$:Tm^{2+} (X = Cl, Br, I) series is presented. The spectroscopic properties of Tm^{2+} are affected by the chemical variation of the compounds. This is ideal to achieve a more thorough understanding of the 4f–5d UC properties of this ion. The samples were studied under the same experimental conditions and we find that the UC efficiency increases along the halide series. The UC mechanism is found to be a combination of the two most prominent UC processes, which involve absorption and energy-transfer steps.

[a] Dr. J. Grimm, E. Beurer, Dr. P. Gerner, Prof. H. U. Güdel
Department of Chemistry and Biochemistry
University of Bern, Freiestrasse 3, 3012 Bern (Switzerland)
Fax: (+41) 31-631-4399
E-mail: hans-ulrich.guedel@iac.unibe.ch

Results

In Figure 1, the 10 K absorption spectra of $CsCaCl_3:Tm^{2+}$, $CsCaBr_3:Tm^{2+}$ and $CsCaI_3:Tm^{2+}$ are displayed. A weak and sharp 4f–4f absorption transition is observed around 8800 cm^{-1} in all three samples. Note the scaling factor for this transition. The position as well as the band shape does not vary much along the series. The energy range extending from 12000 cm^{-1} in the NIR up to the UV region is that in which the 4f–5d transitions of Tm^{2+} occur. The 4f–5d transitions are parity allowed and thus high absorption intensities are observed. The energy gap ΔE between the ($^3H_6$,t_{2g}) and ($^3F_4$,t_{2g}) multiplets, indicated in Figure 1, is relevant for the emission properties and its exact value is given in Table 1 for the three compounds.

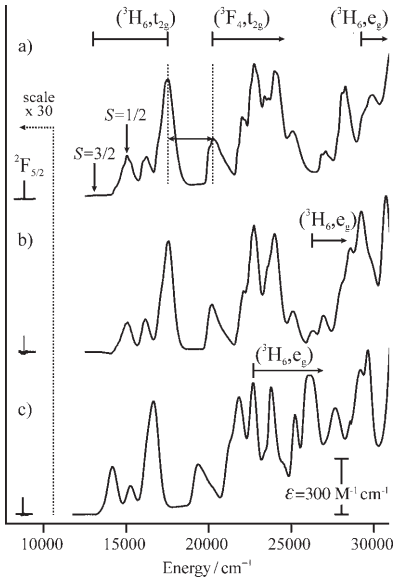

Figure 1. 10 K absorption spectrum of a) $CsCaCl_3$:1.04 % Tm^{2+}, b) $CsCaBr_3$:0.48 % Tm^{2+} and c) $CsCaI_3$:0.76 % Tm^{2+}. The observed absorption transitions in this region are due to the Tm^{2+} 4f–4f and 4f–5d transitions from the $^2F_{7/2}$ ground state. The assignment of the absorption bands is given on top of the $CsCaCl_3:Tm^{2+}$ spectrum. Note the scaling factor for the $^2F_{7/2}\rightarrow{}^2F_{5/2}$ transition. The onset of ($^3H_6$,e_g) is indicated for all three compounds, because the onset of the e_g shifts to lower energies along the series. The energy gap ΔE is between the ($^3H_6$,t_{2g}) and ($^3F_4$,t_{2g}) relevant for the emission properties of the three samples.

Figure 2 shows the 10 K UC emission spectra of the three samples (full lines) and the UC excitation spectra (dotted lines). The number of observed emissions depends on the host lattice. Up to five distinct emission band systems are observed. Emissions C, D and F are the UC emissions, whereas B and A correspond to downconversion emissions. The 10 K maxima of emissions B, C, D and F as well as the origin of emission A are given in Table 1. The assignment of the bands will be discussed later. The UC excitation spectra were obtained by monitoring at the maximum of emission D, while the laser was scanned in the region of the low-energy tail of the ($^3H_6$,t_{2g}) absorption (see Figure 1). The dotted arrow in Figure 2c corresponds to the excitation energy of laser 2 in the two-colour experiment (see below).

Table 1. Compiled data of the spectroscopic properties of $CsCaCl_3:Tm^{2+}$, $CsCaBr_3:Tm^{2+}$ and $CsCaI_3:Tm^{2+}$.[a]

	$CsCaCl_3:Tm^{2+}$	$CsCaBr_3:Tm^{2+}$	$CsCaI_3:Tm^{2+}$
$\hbar\omega_{max}$ [cm^{-1}][b]	310	210	170
ΔE [cm^{-1}]	2760	2620	2700
A [cm^{-1}]	8810	–	8785
B [cm^{-1}]	12497	12237	11348
C [cm^{-1}]	–	–	12703
UC_{exc} [cm^{-1}]	13150	13100	12350
η_{UC} [%][c]	0.1	0.2	11
T_Q (D) [K]	75	125	275
τ (B) [μs][d]	296	323	391
τ (D) [μs][e]	0.9	1.7	1.1
τ_1 (D) UC [μs][e]	19	1.7	3.9
τ_2 (D) UC [μs]	101	26	13.1

[a] $\hbar\omega_{max}$ is the highest vibrational energy in the respective lattice. ΔE is the energy difference between the ($^3F_4$,t_{2g}) and the ($^3H_6$,t_{2g}) absorption multiplets at 10 K, see Figure 1. A denotes the origin of emission A whereas B, C, D and F correspond to the maxima of the respective emissions at 10 K. UC_{exc} is the excitation energy for the UC process. η_{UC} is a measure for the upconversion efficiency at 10 K and is defined in Equation (1). The quenching temperature T_Q(D) is the temperature at which the intensity of the UC emission D drops below 10 % of the intensity at 10 K. The lifetime τ of emissions B and D in downconversion as well as the decay components of emission D in UC are given. [b] From reference [13]. [c] Excitation power density: 4.7 kW cm^{-2}, T = 10 K. [d] Excitation at 21834 cm^{-1}, from reference [13]. [e] Excitation at 28195 cm^{-1}, from reference [13].

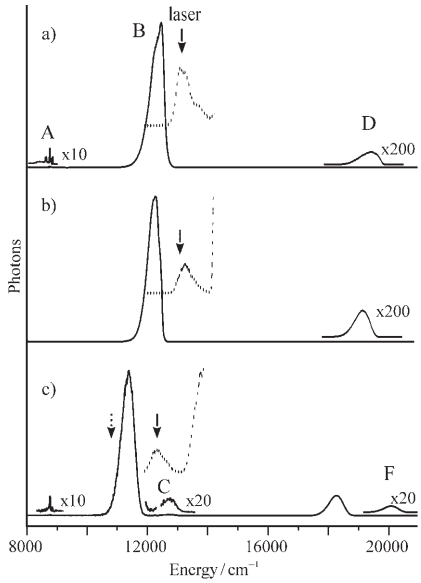

Figure 2. Overview UC emission spectra at 10 K of a) $CsCaCl_3$:1.04 % Tm^{2+}, b) $CsCaBr_3$:0.48 % Tm^{2+} and c) $CsCaI_3$:0.76 % Tm^{2+} photoexcited at 13150, 13100 and 12350 cm^{-1}, respectively, see full arrows. The excitation power density was 4.7 kW cm^{-2} for all spectra. The labelling of the emission bands is given on top of the $CsCaCl_3:Tm^{2+}$ and $CsCaI_3:Tm^{2+}$ spectra. Note the scaling factors for the various emission bands. The insets (dotted lines) correspond to the 10 K UC excitation scans of a) $CsCaCl_3:Tm^{2+}$ monitored at 19450 cm^{-1}, b) $CsCaBr_3:Tm^{2+}$ monitored at 19070 cm^{-1} and c) $CsCaI_3:Tm^{2+}$ monitored at 18250 cm^{-1}. The dotted arrow in c) corresponds to the excitation energy of laser 2 in the two-colour experiment.

In Figure 3, the intensity of emissions D and B of $CsCaI_3:Tm^{2+}$ is shown in a double logarithmic representation as a function of the exciting laser power in an UC experiment. Emission D depends quadratically on the laser power as evidenced by the slope of 1.93 obtained from a fit of the data (Figure 3a). In contrast, emission B shows a linear dependence on the laser power, with a slope of 0.92 (Figure 3b). The same experiment yields slopes of 1.8 and 1.7 for emission D in $CsCaCl_3:Tm^{2+}$ and $CsCaBr_3:Tm^{2+}$, respectively, and 1.1 for emission B in $CsCaBr_3:Tm^{2+}$ (data not shown).

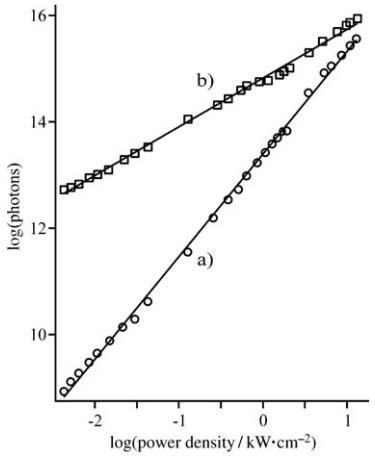

Figure 3. Excitation power dependence of the number of emitted photons at 10 K in a double-logarithmic representation: a) visible UC emission band D and b) NIR emission band B of $CsCaI_3:Tm^{2+}$. Laser excitation of the sample occurred at 12350 cm^{-1}. The straight lines correspond to linear fits to the logarithmic data with slopes of a) 1.93 and b) 0.92.

Figure 4 shows the temporal evolution of the 10 K luminescence intensity of emission D in the three samples after 10 ns excitation pulses at 14450 cm^{-1} into the ($^3H_6$,t_{2g}) multiplet. All three curves can be fitted by double exponential decay functions and the decay times are given in Table 1. The decay curves are relevant for the identification of the upconversion mechanism and will be discussed later.

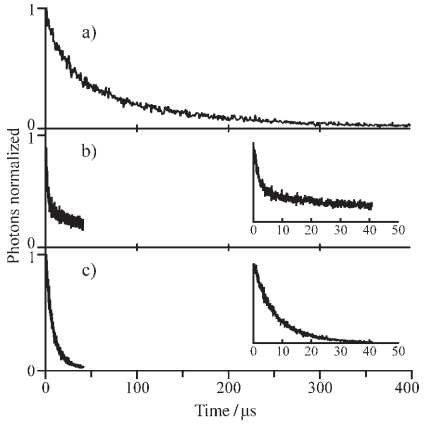

Figure 4. Time evolution of emission D at 10 K after 10 ns pulsed excitation at 14450 cm^{-1} in a) $CsCaCl_3:Tm^{2+}$, b) $CsCaBr_3:Tm^{2+}$ and c) $CsCaI_3:Tm^{2+}$. The insets in b) and c) show the same data on an expanded time scale.

In Figure 5, the intensity of the UC emission D of $CsCaI_3:Tm^{2+}$, monitored at 18250 cm^{-1}, is shown for various combinations of two exciting lasers. In this two-colour experiment, a Ti-sapphire laser (laser 1) was used to pump at 12350 cm^{-1} (full arrow in Figure 2c). At this energy, Tm^{2+} ground-state absorption occurs into the ($^3H_6$,t_{2g}) multiplet and thus Tm^{2+} UC is induced (Figure 5). Laser 2 was used to pump at 10800 cm^{-1}, which is below the onset of ($^3H_6$,t_{2g}) absorption (dotted arrow in Figure 2c). This laser alone induces no upconversion emission D as can be seen from a comparison of Figure 5c, in which the intensity of emission D is at the dark-count level. The combination of the two lasers results in a more than twofold increase of the UC emission compared to the sum of the UC intensity of the two individual lasers, see Figure 5a and b. This result will be discussed together with the transients (Figure 4) in connection with the upconversion mechanism.

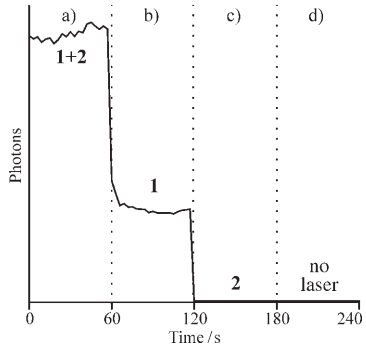

Figure 5. Intensity of emission D in the two-colour laser UC experiment in $CsCaI_3:Tm^{2+}$ with laser 1 at 12350 cm^{-1} (0.34 kW cm^{-2}), see full arrow in Figure 2c, and laser 2 at 10800 cm^{-1} (8.3 kW cm^{-2}), see dotted arrow in Figure 2c. The sequence corresponds to the following combinations of the lasers: a) lasers 1 and 2, b) only laser 1, c) only laser 2, d) both lasers blocked.

Discussion

Materials and site symmetries: $CsCaCl_3$ and $CsCaBr_3$ are cubic perovskites at room temperature that crystallise in the *Pm3m* space group.[15,16] Tm^{2+} replaces Ca^{2+} on a crystallographic site with O_h point symmetry. Upon cooling both samples undergo phase transitions. The site symmetry of Ca^{2+} below the phase change is C_{4h} in $CsCaCl_3$.[17] At 10 K $CsCaBr_3$ crystallises in the orthorhombic *Pnma* phase, which is the phase that is also found for $CsCaI_3$ in the temperature range between 10 and 300 K.[18] The Ca^{2+} ion in the orthorhombic *Pnma* phase has site symmetry *Ci*. Regardless of the phase changes, the Tm^{2+} ion is always coordinated by six X^- ions ($X^- = Cl$, Br, I). From the spectroscopic data of the three samples we conclude that the only band splitting due to symmetry reduction is observable in the 4f–4f transi-

tions and is in the order of a few wavenumbers.[13] The data interpretation is therefore done in the octahedral approximation.

Assignment of states: The assignment of the excited states and the emission bands has already been discussed for the three compounds in references [13,19]. A brief recapitulation is given here. Figure 6 shows the energy level diagram of the spectroscopically relevant excited states of Tm^{2+} as well as the observed transitions.

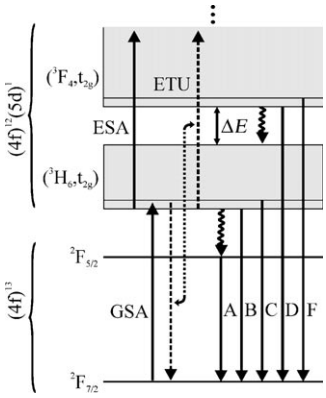

Figure 6. Schematic energy-level diagram for Tm^{2+}-doped $CsCaCl_3$, $CsCaBr_3$ and $CsCaI_3$ with the relevant radiative (straight arrows) and nonradiative processes (curly and dotted arrows). GSA, ESA and ETU stand for ground-state absorption, excited-state absorption and energy-transfer upconversion, respectively. They are the relevant processes in UC. The energy gap ΔE is indicated in Figure 1. The labelling of the emission bands corresponds to Figure 2 and the electronic transitions to which they refer are explained in the text.

Tm^{2+} has a $(4f)^{13}$ ground-state electron configuration, that is, it corresponds to a one 4(f) hole system and is isoelectronic with Yb^{3+}. There are only two multiplets arising from the $(4f)^{13}$ electron configuration, which are the $^2F_{7/2}$ ground state and the $^2F_{5/2}$ first excited state. The sharp 4f–4f transitions are observed in absorption and emission (labelled A) around 8800 cm^{-1}; see Figures 1 and 2.

In the absorption spectra of Figure 1, all bands above 10000 cm^{-1} are due to 4f–5d transitions. They are between one and four orders of magnitude more intense than the intraconfigurational 4f–4f transitions, because they are parity-allowed.[20–22] The excited states arise from the $(4f)^{12}(5d)^1$ electron configuration. This has a total degeneracy of 910, and energy splittings occur as a result of various interactions.

An important interaction in the $(4f)^{12}(5d)^1$ configuration is the ligand-field interaction of the 5d electron. The octahedral ligand field splits the 5d orbitals into t_{2g} and e_g sets, separated by 10 Dq. The octahedral (O_h) coordination of Tm^{2+} in all three samples causes the t_{2g} to be lower in energy than the e_g. The $(4f)^{12}$ part is split into the $^{2S+1}L_J$ terms of Tm^{3+} by the Coulomb repulsion and the spin-orbit coupling of the 4f electrons. Thus, the energy multiplets of the Tm^{2+} $(4f)^{12}(5d)^1$ configuration can be roughly characterised as $(^{2S+1}L_J,t_{2g})$ and $(^{2S+1}L_J,e_g)$, see Figure 1. For Tm^{2+} we expect each of these multiplets to be split into a set of high-spin $S=3/2$ and a set of low-spin $S=1/2$ states due to the isotropic exchange part of the Coulomb interaction between the 4f and 5d electrons. Due to Hund's rule, the former lie lower in energy. As a consequence, transitions from the $^2F_{7/2}$ ground state to the lowest energy 4f–5d states are expected to have formally spin-forbidden character. This is expressed in weaker oscillator strengths compared to the spin-allowed bands.[20,22,23] The first spin-forbidden and spin-allowed bands are marked with vertical arrows in Figure 1.

The 5d–4f emission bands in Figure 2 are assigned to the following transitions: Band B is a spin-forbidden 5d–4f transition from $(^3H_6,t_{2g})$ $S=3/2$ to $^2F_{7/2}$. The corresponding weak absorption band is hardly seen in Figure 1, but clearly observable in the UC excitation spectra in Figure 2. In $CsCaI_3:Tm^{2+}$ a spin-allowed emission from the first $(^3H_6,t_{2g})$ $S=1/2$ state to the ground state is observed and labelled emission C. Band D is assigned to a transition from the lowest excited state of the $(^3F_4,t_{2g})$ multiplet to the $^2F_{7/2}$ ground state. The spin of the emitting $(^3F_4,t_{2g})$ state is not specified, because spin ceases to be a good quantum number in the higher multiplets.[13,24] In $CsCaI_3:Tm^{2+}$, a very weak emission F at energies higher than emission D is observed, originating in a higher excited state of the $(^3F_4,t_{2g})$ multiplet. A schematic picture of these radiative transitions is given in Figure 6.

4f–5d to 4f–5d upconversion in Tm^{2+}: Excitation into the spin-forbidden component of the $(^3H_6,t_{2g})$ leads to the observation of multiple luminescences in the title compounds at 10 K, see Figure 2. Emission D is the dominant UC luminescence in all three samples. The intensity of emission D depends quadratically on the excitation power, see Figure 3a. This confirms that it is created by a two-photon excitation. At 10 K the large size of the energy gap ΔE prevents efficient multiphonon relaxation from $(^3F_4,t_{2g})$ to $(^3H_6,t_{2g})$, especially in the bromide and iodide, see also reference [13]. Most of the energy in $(^3F_4,t_{2g})$ is therefore emitted radiatively in emission band D in a bromide and iodide environment.

For excitation into the $(^3H_6,t_{2g})$ $S=3/2$ multiplet, emission B dominates the emission spectrum in all samples at 10 K. This is not surprising, because direct pumping in the $(^3H_6,t_{2g})$ $S=3/2$ absorption band occurs. The intensity of emission B depends linearly on power (Figure 3b). Multiphonon relaxation from $(^3H_6,t_{2g})$ $S=3/2$ to $^2F_{5/2}$ populates the $^2F_{5/2}$ multiplet (see curly arrow in Figure 6). Emission A, which originates in this state, is very weak in the chloride and iodide, yet is not observed at 10 K in the bromide. It does come up with temperature in the latter, but only above 130 K. Thus, the $(^3H_6,t_{2g})$ $S=3/2$ multiplet serves as the important intermediate level for the UC process, see also Figure 6.

The emission properties were also studied as a function of temperature under UC excitation. The intensity of emission D decreases with increasing temperature in all samples.

However, the quenching temperatures T_Q(D) are different for the three samples as can be seen from Table 1. We define T_Q(D) as the temperature at which the intensity of band D drops below 10% of the intensity at 10 K. T_Q(D) increases along the series. This trend is also observed for downconversion excitation where the quenching of emission D occurs at similar temperatures.[13] The shift of T_Q(D) to higher temperatures is ascribed to the decreased phonon energies along the series, see Table 1.

Upconversion mechanisms: The temporal behaviour of the UC luminescence after short-pulse excitation is used to assign the mechanisms that enable the UC. The two most prominent UC mechanisms are a sequence of ground-state absorption (GSA) and excited-state absorption (ESA) steps or GSA followed by an energy-transfer step (ETU). GSA/ESA is usually a one-ion process, whereas GSA/ETU is a two-ion process. The signature of the former is an immediate decay of the UC emission after the excitation pulse, whereas for the latter the decay is preceded by a rise.[25] Both mechanisms are indicated on the left-hand side of Figure 6. Direct excitation into the 4f–5d absorption bands above ($^3F_4$,t_{2g}) with short pulses yields single exponential decay curves of both emissions B and D, and their lifetimes are included in Table 1.

The transients of emission D excited by UC reproduced in Figure 4 show an immediate decay after the termination of the laser pulse for all three compounds. This is indicative of a dominant GSA/ESA mechanism. The two-colour experiment for the iodide shown in Figure 5 provides unambiguous evidence for the existence of a GSA/ESA process. One would not expect to see a difference between the light levels in Figure 5a and b if GSA/ETU was the dominant mechanism. In the UC experiments, there will also be a contribution from a $^2F_{5/2}\rightarrow(^3F_4,t_{2g})$ UC process. However, this process will be active in both, the one-colour (Figures 2 and 5b) and two-colour experiments (Figure 5a). We therefore exclude that this process accounts for the differences in intensity between Figure 5a and b. A decay component that is more than an order of magnitude longer than the lifetime of emission D measured under direct excitation is also present in all three compounds (Figure 4 and Table 1). This points to the co-existence of a GSA/ETU mechanism, with a decay time governed by the lifetime of the intermediate excited state ($^3H_6$,t_{2g})S = 3/2. The UC transients thus bear the signature of both the GSA/ESA and the GSA/ETU mechanism, with the former dominating (see Figure 6). Because no direct correlation between the lifetimes measured in downconversion and the UC transients can be made, the existence of several UC species in all samples is inferred. Very often a subset of the luminescent ions, which may be different from the main species observed in downconversion luminescence, dominates in upconversion.[26]

Upconversion efficiency: The intensity distribution among the observed emission bands is very different in the three title compounds. This leads to very different efficiencies for the UC process. The efficiency of the UC process is defined in Equation (1).

$$\eta_{UC} = \frac{\text{Photons}_{Vis}}{2\,\text{Photons}_{Vis} + \text{Photons}_{NIR}} \quad (1)$$

To evaluate this ratio, it is important to plot the UC luminescence spectra as number of photons (not intensity) versus wavenumbers, as is done in Figure 2. The integrated emission bands then correspond to the number of photons that can be inserted in Equation (1). Efficiencies were determined from spectra measured under identical conditions in order to allow comparison. The UC efficiencies at 10 K for a laser power density of 4.7 kW cm^{-2} are listed in Table 1. The efficiency in $CsCaCl_3$:Tm^{2+} and $CsCaBr_3$:Tm^{2+} is very low, whereas that of the iodide is very high, also in comparison with established upconverters.[27] This increase of UC in the iodide by two orders of magnitude compared to the chloride and bromide cannot be fully accounted for by the reduced loss processes due to hindered multiphonon relaxation. As shown in Figure 1, the iodide shows a significant difference in the absorption spectrum and thus in the energy level structure of the f–d states in the region above 20000 cm^{-1}. As a result of the smaller 10 Dq value of the 5d electron in the iodide, the first 4f to 5d(e_g) absorption occurs as low as 22300 cm^{-1}, see Figure 1. As a consequence, both the ESA and the ETU step in the UC processes with 12350 cm^{-1} excitation correspond to a 5d(t_{2g})→5d(e_g) excitation in the iodide. In the chloride and bromide, on the other hand, the ($^3H_6$,e_g) multiplet lies above 26000 cm^{-1} and thus the ESA and ETU step in the ($^3H_6$,t_{2g})→($^3F_4$,t_{2g}) UC process correspond to a 4f–4f excitation. This 4f–4f excitation has an oscillator strength, which is one to two orders of magnitude lower than the than the 5d(t_{2g})→5d(e_g) excitation in the iodide.[28] We can thus explain the impressingly high UC efficiency in $CsCaI_3$:Tm^{2+}.

Conclusion

The experimental findings clearly show the existence of upconversion processes between the 4f–5d states of Tm^{2+} in the title compounds. This type of UC is without precedent. Usually, rapid multiphonon relaxation between the 4f–5d states prevents emission from higher excited 4f–5d states. In the title compounds the observation of more than one 5d–4f emission is made possible by the favourable energy-level structure of the 4f–5d states with a large energy gap ΔE between the ($^3F_4$,t_{2g}) and ($^3H_6$,t_{2g}) multiplets. Other important factors for the observation of emission D are the low phonon energies of the lattices, particularly in the bromide and iodide. The present study demonstrates that UC processes are not restricted to 4f–4f transitions in lanthanides and some special cases of transition metal doped materials. These results also demonstrate the power of chemical variation. It is only by the comparison of the three systems that

we are able to identify and characterise the relevant UC mechanisms.

Experimental Section

Synthesis and crystal growth: Single crystals of $CsCaCl_3$, $CsCaBr_3$ and $CsCaI_3$ doped with Tm^{2+} were grown by the Bridgman technique. For the synthesis, stoichiometric amounts of CsX (X = Cl, Br, I) and CaX_2 were mixed. Tm^{2+} was prepared in situ by synproportionation of TmX_3 (prepared by the ammonium halide route from 99.999% pure Tm_2O_3 from Johnson Matthey) and Tm metal (Alfa Aesar 99.9%).[29] The absolute concentration of Tm in the crystals was determined with inductively coupled plasma-optical emission spectroscopy (ICP-OES) and is 1.04, 0.48 and 0.76% in $CsCaCl_3$, $CsCaBr_3$ and $CsCaI_3$, respectively. The use of tantalum rather than the more commonly used silica ampoules is indispensable for obtaining crystals that contain no Tm^{3+}. Crystals grown from silica ampoules contain trace amounts of Tm^{3+}, because under such crystal growth conditions Tm^{2+} is easily oxidised by silica. Due to the hygroscopic nature of the starting materials as well as the crystals, the handling occurred under inert atmosphere at all times. For absorption measurements the samples were polished in a dry box and enclosed in an airtight copper cell. Thermal contact of the crystal with the sample holder was provided through application of copper grease (Lake Shore Cryotronics). For luminescence measurements, the samples were sealed into quartz ampoules under partial pressure of He, which serves as an inert atmosphere as well as a heat transmitter.

Spectroscopic measurements: Sample cooling was achieved with a closed-cycle cryostat (Air Products) for absorption and with the He gas flow technique for emission measurements. Absorption spectra were recorded on a Cary 6000i spectrometer (Varian).

For upconversion luminescence measurements, the samples were excited with one or two multimode standing wave Ti:sapphire lasers (Spectra Physics 3900S), pumped by the second harmonic of a $Nd:YVO_4$ laser (Spectra Physics Millennia Xs) or by an argon-ion laser in all-lines mode (Spectra Physics 2045–15/4S). The wavelength control of the Ti:sapphire laser was achieved by an inchworm-driven (Burleigh PZ-501) birefringent filter and a wavemeter (Burleigh WA2100). The sample luminescence was dispersed either with a 0.85 m double monochromator (Spex 1402) or a 0.75 m single monochromator (Spex 1702). A cooled PMT (Hamamatsu P3310–01) and a photon counting system (Stanford Research 400) or a Ge detector (ADC 403 L) interfaced to a lock-in amplifier (Stanford Research 830) were used for the detection of the signal in the visible and infrared range, respectively. The laser power was measured with a power meter (Coherent Labmaster Ultima) and the laser beam was focused using a $f = 53$ mm lens. The typical excitation density was 4.7 $kW\,cm^{-2}$ for the one-colour upconversion experiments. The excitation densities used for the two-colour upconversion experiments were of the order of 0.34 $kW\,cm^{-2}$ for laser 1 and about 8.3 $kW\,cm^{-2}$ for laser 2. To measure the power dependence, the beam was attenuated with a series of neutral density filters (Balzers). For time-resolved measurements 10 ns pulses of the second harmonic of a Nd:YAG (Quanta Ray DCR 3, 20 Hz) pumped dye laser (Lambda Physik FL 3002; pyridine 1 in methanol) were used. Transient signals were detected as described above using a multichannel scaler (Stanford Research 430).

All luminescence spectra are corrected for the sensitivity of the detection system and are displayed as photon counts versus energy.[30]

Acknowledgements

We thank A. Aebischer and J. F. Suyver for valuable discussions. The Swiss National Science Foundation is gratefully acknowledged for financial support.

[1] F. Auzel, *Chem. Rev.* **2004**, *104*, 139–173.
[2] J. F. Suyver, A. Aebischer, D. Biner, P. Gerner, J. Grimm, S. Heer, K. Krämer, C. Reinhard, H. U. Güdel, *Opt. Mater.* **2005**, *27*, 1111–1130.
[3] M. F. Joubert, *Opt. Mater.* **1999**, *11*, 181–203.
[4] M. L. F. Phillips, M. P. Hehlen, K. Nguyen, J. M. Sheldon, N. J. Cockroft, *Proc. Electrochem. Soc.* **2000**, *99-40*, 123–129.
[5] S. Heer, K. Kömpe, M. Haase, H. U. Güdel, *Adv. Mater.* **2004**, *16*, 2102–2105.
[6] A. Shalav, B. S. Richards, T. Trupke, K. W. Krämer, H. U. Güdel, *Appl. Phys. Lett.* **2005**, *86*, 013505.
[7] O. S. Wenger, D. R. Gamelin, H. U. Güdel, *J. Am. Chem. Soc.* **2000**, *122*, 7408–7409.
[8] M. Wermuth, H. U. Güdel, *Chem. Phys. Lett.* **1997**, *281*, 81–85.
[9] A. Aebischer, G. M. Salley, H. U. Güdel, *J. Chem. Phys.* **2002**, *117*, 8515–8522.
[10] W. J. Schipper, A. Meijerink, G. Blasse, *J. Lumin.* **1994**, *62*, 55–59.
[11] C. Wickleder, *J. Alloys Compd.* **2000**, *300–301*, 193–198.
[12] O. S. Wenger, C. Wickleder, K. W. Krämer, H. U. Güdel, *J. Lumin.* **2001**, *94–95*, 101–105.
[13] J. Grimm, J. F. Suyver, E. Beurer, G. Carver, H. U. Güdel, *J. Phys. Chem. A* **2006**, *110*, 2093–2101.
[14] E. Beurer, J. Grimm, P. Gerner, H. U. Güdel, *J. Am. Chem. Soc.* **2006**, *128*, 3110–3111.
[15] H. J. Seifert, U. Langenbach, *Z. Anorg. Allg. Chem.* **1969**, *368*, 36–43.
[16] H. J. Seifert, D. Haberhauer, *Z. Anorg. Allg. Chem.* **1982**, *491*, 301–307.
[17] Y. Vaills, J. Y. Buzaré, A. Gibaud, C. Lunay, *Solid State Commun.* **1986**, *60*, 139.
[18] G. Schilling, G. Meyer, *Z. Anorg. Allg. Chem.* **1996**, *622*, 759–765.
[19] J. Grimm, E. Beurer, H. U. Güdel, *Inorg. Chem.* **2006**, in press.
[20] D. S. McClure, Z. J. Kiss, *J. Chem. Phys.* **1963**, *39*, 3251–3257.
[21] L. van Peterson, M. F. Reid, R. T. Wegh, S. Soverna, A. Meijerink, *Phys. Rev. B* **2002**, *65*, 045114.
[22] L. van Peterson, M. F. Reid, R. T. Wegh, G. W. Burdick, A. Meijerink, *Phys. Rev. B* **2002**, *65*, 045114.
[23] P. Dorenbos, *J. Phys. Condens. Matter* **2003**, *15*, 575–594.
[24] P. Dorenbos, *J. Phys. Condens. Matter* **2003**, *15*, 6249.
[25] D. R. Gamelin, H. U. Güdel, *Top. Curr. Chem.* **2001**, *214*, 1–56.
[26] S. Garcia-Revilla, P. Gerner, O. S. Wenger, H. U. Güdel, R. Valiente, *Chem. Phys. Lett.* **2005**, *401*, 492–496.
[27] J. F. Suyver, J. Grimm, K. W. Krämer, H. U. Güdel, *J. Lumin.* **2005**, *114*, 53–59.
[28] B. Henderson, G. F. Imbusch, *Optical Spectroscopy of Inorganic Solids*, Oxford Science, Oxford, **1989**.
[29] G. Meyer, *Inorg. Synth.* **1989**, *25*, 146–150.
[30] E. Ejder, *J. Opt. Soc. Am.* **1969**, *59*.

Received: March 27, 2006
Published online: October 26, 2006

